Molecular Cell
Article

HAT4, a Golgi Apparatus-Anchored B-Type Histone Acetyltransferase, Acetylates Free Histone H4 and Facilitates Chromatin Assembly

Xiaohan Yang,[1] Wenhua Yu,[1] Lei Shi,[1] Luyang Sun,[1] Jing Liang,[1] Xia Yi,[1] Qian Li,[1] Yu Zhang,[1] Fen Yang,[1] Xiao Han,[1] Di Zhang,[1] Jie Yang,[2] Zhi Yao,[2] and Yongfeng Shang[1,2,*]
[1]Key Laboratory of Carcinogenesis and Translational Research (Ministry of Education), Department of Biochemistry and Molecular Biology, Peking University Health Science Center, Beijing 100191, China
[2]Tianjin Key Laboratory of Medical Epigenetics, Tianjin Medical University, Tianjin 300070, China
*Correspondence: yshang@hsc.pku.edu.cn or yshang@tijmu.edu.cn
DOI 10.1016/j.molcel.2011.07.032

SUMMARY

Histone acetyltransferases (HATs) are an essential regulatory component in chromatin biology. Unlike A-type HATs, which are found in the nucleus and utilize nucleosomal histones as substrates and thus primarily function in transcriptional regulation, B-type HATs have been characterized as cytoplasmic enzymes that catalyze the acetylation of free histones. Here, we report on a member of the GCN5-related N-acetyltransferase superfamily and another B-type HAT, HAT4. Interestingly, HAT4 is localized in the Golgi apparatus and displays a substrate preference for lysine residues of free histone H4, including H4K79 and H4K91, that reside in the globular domain of H4. Significantly, HAT4 depletion impaired nucleosome assembly, inhibited cell proliferation, sensitized cells to DNA damage, and induced cell apoptosis. Our data indicate that HAT4 is an important player in the organization and function of the genome and may contribute to the diversity and complexity of higher eukaryotic organisms.

INTRODUCTION

The enzymes that catalyze the acetylation of free but not nucleosomal histones are called B-type HATs or B-HATs. B-HATs are distinct from A-type HATs or A-HATs, which act on histones that have already been incorporated into chromatin (Richman et al., 1988). To date, only a few B-HATs have been characterized, including HAT1 for H4K5/12 (Parthun et al., 1996), Rtt109 for H3K9/27/56 (Burgess et al., 2010; Fillingham et al., 2008), and HatB3.1 for H3 in yeast (Sklenar and Parthun, 2004). Among them, HAT1 is the only B-HAT that is conserved from yeast to human (Ge et al., 2011; Parthun, 2007). Known as a classical example of a type B histone acetyltransferase, HAT1 catalyzes the acetylation of the histone H4 tail at H4K5 and H4K12, with HAT2 (yeast homolog of human RbAp48) as an essential cofactor (Parthun et al., 1996). Although the subcellular localization of HAT1 appears to be dynamically regulated throughout development, since no A-HATs have been shown to be in the cytoplasm, cytoplasmic localization, primarily but maybe not exclusively, is still considered to be a distinct characteristic of B-HATs (Parthun, 2007). Structurally, HAT1 is a paradigm of the GCN5 (*G*eneral *C*ontrol *N*onderepressible *5*)-related N-acetyltransferase superfamily (Dutnall et al., 1998), and, functionally, a spectrum of phenotypes observed in the absence of *HAT1* is consistent with a role for its protein in chromatin organization (Parthun, 2007). However, surprisingly, neither the highly conserved pattern of acetylation on newly synthesized histone H4 nor the equally well conserved HAT1 itself is necessary for the viability of yeast (Parthun, 2007), leading to the suggestion that there might be additional histone acetyltransferases that overlap functionally with HAT1 to modify newly synthesized histone H4.

Here, we report on another B-HAT, HAT4. We showed that HAT4 is primarily localized in the Golgi apparatus and preferentially acetylates free histone H4, but in its globular domain. We showed that HAT4 is involved in nucleosome formation and chromatin organization and that it is required for normal growth and homeostasis of cells.

RESULTS

Cloning and Characterization of HAT4

In an effort to identify more histone modifiers that are potentially involved in gene regulation, we cloned a gene from a mammary library (Clontech). The cDNA of this gene (NM_024845.2) is 729 bp in length, with an open reading frame encoding for a protein of 243 amino acids (Figure 1A). The corresponding gene is mapped to chromosome 16p13.3 consisting of five exons and four introns, which transcribes a message in multiple tissues according to data from UniGene (http://www.genecards.org) (Figure 1B). The predicted molecular weight of this protein is 27 kDa. Real-time reverse transcriptase (RT) PCR analysis of the mRNA expression and western blotting examination of the protein expression using polyclonal antibodies against HAT4 that we generated in rabbits with recombinant HAT4 protein showed that endogenous HAT4 is broadly expressed in a collection of cell lines and that it is a protein of approximately 27 kDa (Figure 1C), confirming its predicted molecular weight. Structural

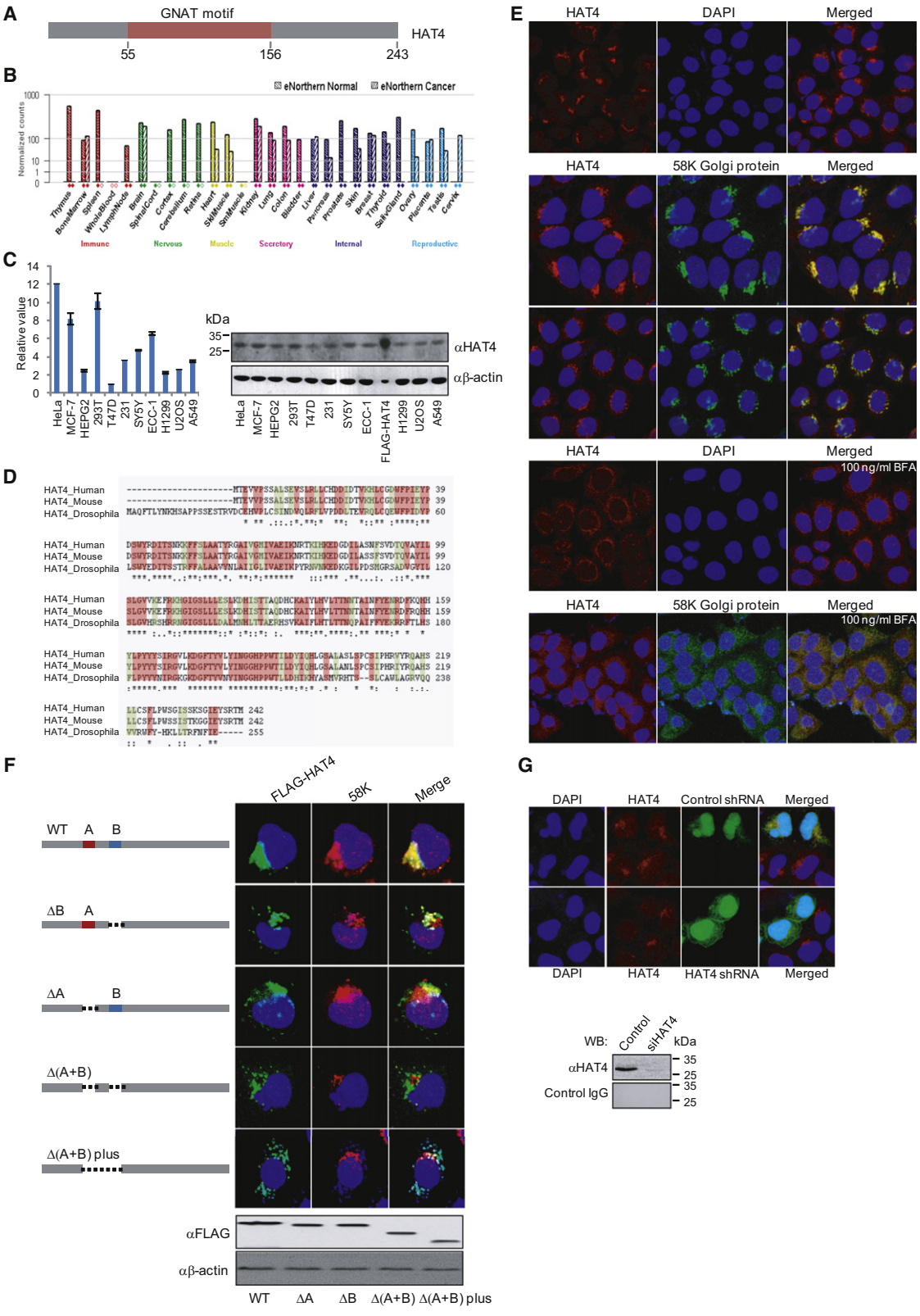
A
GNAT motif
HAT4
55
156
243
B
eNorthern Normal
eNorthern Cancer
Normalized counts
Thymus
BoneMarrow
Spleen
WholeBlood
LymphNode
Brain
SpinalCord
Cortex
Cerebellum
Retina
Heart
SkMuscle
SmMuscle
Kidney
Lung
Colon
Bladder
Liver
Pancreas
Prostate
Skin
Breast
Thyroid
SalivGland
Ovary
Placenta
Testis
Cervix
Immune
Nervous
Muscle
Secretory
Internal
Reproductive
C
Relative value
HeLa
MCF-7
HEPG2
293T
T47D
231
SY5Y
ECC-1
H1299
U2OS
A549
kDa
35
25
αHAT4
αβ-actin
FLAG-HAT4
D
HAT4_Human
HAT4_Mouse
HAT4_Drosophila
E
HAT4
DAPI
Merged
58K Golgi protein
100 ng/ml BFA
F
FLAG-HAT4
58K
Merge
WT
A
B
ΔB
ΔA
Δ(A+B)
Δ(A+B) plus
αFLAG
αβ-actin
WT
ΔA
ΔB
Δ(A+B)
Δ(A+B) plus
G
Control shRNA
HAT4 shRNA
WB:
Control
siHAT4
αHAT4
Control IgG

analysis revealed that this protein contains only one putative functional domain, a GCN5-related N-acetyltransferase motif (55–156 amino acids) (Figure 1A). We named this protein "HAT4" after HAT1, HAT2, and HatB3.1. Amino acid sequence alignment indicated that human HAT4 shares 97% identity with its mouse homolog, NP_083366, and 55% similarity with its *Drosophila* homologs (Figure 1D); there are two isoforms in *Drosophila* which are named Hat4a (NP_996032.1) and Hat4b (NP_648353.3), respectively.

To gain insight into the biological function of the HAT4 protein, we first analyzed its subcellular localization. Exponentially growing HeLa cells were fixed and immunostained with HAT4 antibodies. Immunofluorescent imaging revealed a highly reproducible perinuclear distribution pattern for HAT4 (Figure 1E). This pattern is reminiscent of the cellular distribution pattern of the Golgi apparatus. In order to investigate the possibility that HAT4 is localized in the Golgi apparatus, HeLa cells were double immunostained with anti-HAT4 and anti-58K Golgi protein (Saraste et al., 1987). The results showed that HAT4 and the Golgi apparatus marker are indeed colocalized inside HeLa cells (Figure 1E). In addition, treatment of HeLa cells with brefeldin A, an inhibitor of intracellular protein transport that could cause the disassembly of the Golgi apparatus (Fujiwara et al., 1988), led to a diffused pattern of distribution of HAT4 and the 58K Golgi protein in the cytoplasm (Figure 1E), further supporting the colocalization of HAT4 and the Golgi apparatus.

Although characterized as the machinery for protein post-translational modification, the Golgi apparatus has not previously been reported to harbor any HATs. Nevertheless, bioinformatics analysis indicated that HAT4 possesses potential transmembrane domains in its N-terminal region. Indeed, deletion of these domains led to a dispersion of HAT4 in the cytoplasm (Figure 1F), indicating a dislodgement of HAT4 from the Golgi apparatus and suggesting that HAT4 might be anchored on the Golgi apparatus. The specificity of HAT4 antibodies was verified by western blotting and immunofluorecent staining of HeLa cells with HAT4 knockdown by its specific siRNA or shRNA (Wang et al., 2009; Wu et al., 2005) (Figure 1G).

HAT4 Possesses HAT Activity on Free, but Not Nucleosomal, Histones

In order to determine whether HAT4 indeed possesses HAT activity, bacterially expressed recombinant HAT4 (reHAT4) or immunopurified FLAG-HAT4 from HeLa cells was incubated in the presence of [^{3}H]acetyl-CoA with calf thymus histones or nucleosomal histones that we isolated from HeLa cells. The results of these experiments revealed that, while reHAT4 indiscriminately acetylated all histone species when calf thymus histones were used as the substrates (Figure 2A), HAT4 purified from mammalian cells exhibited an enzymatic preference for histone H4 when incubated with the same substrates (Figure 2B). No HAT activity was detected when nucleosomal histones were used as substrates, regardless of whether HAT4 was from bacteria or mammalian cells, although the nucleosomal histones in our experiments could be efficiently acetylated by pCAF, an A-HAT (Figures 2A and 2B).

In the midst of the GNAT motif of HAT4, there lies an invariant Arg/Gln-X-X-Gly-X-Gly/Ala segment (X denotes variation), R-K-H-G-I-G, which is the acetyl-CoA binding site highly conserved among acetyltransferases (Wolf et al., 1998). It has been reported that mutation of one or more of these three conserved residues dramatically reduces in vitro N-acetyltransferase activity of human spermidine/spermine N^1-acetyltransferase (Lu et al., 1996). To further analyze the HAT activity of HAT4, we generated HAT4G111A mutant to convert the highly conserved glycine to alanine using site-specific mutagenesis. Indeed, HAT4G111A mutant purified from either bacterial or mammalian cells showed dramatic loss of HAT activity (Figure 2C).

As H2A and H2B from calf thymus were hardly distinguishable on SDS-PAGE, we also utilized full-length *Xenopus* histone recombinants purified from BL21 bacteria as substrates for HAT activity assays. Another advantage of these histones is that they are readily purified to homogeneity and are largely underacetylated (Luger et al., 1997). Consistent with the results obtained with calf thymus histones, we found that *Xenopus* histones H2A, H2B, H3, and H4 could be acetylated by recombinant HAT4 from bacteria, whereas HAT4 purified from mammalian cells preferentially acetylated H4 (Figure 2D). In addition, we also cloned *Drosophila Hat4a* and *Hat4b*, purified GST-tagged

Figure 1. Cloning and Characterization of HAT4

(A) Schematic representation of the structure of HAT4 protein.

(B) *HAT4* transcribes in multiple normal and cancer tissues. Electronic Northern: For the set of nonfetal normal and cancer human tissues shown, NCBI's UniGene dataset is mined for information about the number of unique clones per gene per tissue. Clones are assigned to particular tissues by applying data-mining heuristics to UniGene's library information file. Electronic expression results were calculated by dividing the number of clones per gene by the number of clones per tissue. They were then normalized by multiplying by 1M, and the obtained normalized counts are presented on the same root scale as the experimental tissue vectors.

(C) Real-time RT-PCR and western blotting analysis of HAT4 expression in different cancer cell lines. GAPDH or β-actin was analyzed as an internal control. Each bar represents the mean ± SD for three independent experiments.

(D) Amino-acid sequence alignment of HAT4 from different species. The same amino acids are starred and shown in red, and the conserved amino acids are shown in green and marked with two points.

(E) Subcellular localization of HAT4 protein. HeLa cells on coverslips were stained with anti-HAT4 or double stained with anti-HAT4 and anti-58K Golgi protein with or without brefeldin A (BFA) treatment.

(F) Subcellular localization of HAT4 and HAT4 mutants. HeLa cells were transfected with FLAG-HAT4 or FLAG-HAT4 mutants (WT: wild-type; ΔA: deletion of transmembrane region A [52–69aa]; ΔB: deletion of transmembrane region B (84–103aa); Δ(A+B) plus: deletion of transmembrane regions A and B and the amino acids between [52–103aa]) and double stained with anti-FLAG and anti-58K Golgi protein. The expression of FLAG-HAT4 deletion mutants was analyzed by western blotting.

(G) HeLa cells were transfected with control or HAT4 siRNA or HAT4 shRNA plasmids together with green fluorescent protein as a transfection efficiency monitor. Western blotting and immunofluorescent imaging were performed to verify the specificity of anti-HAT4 antibodies.

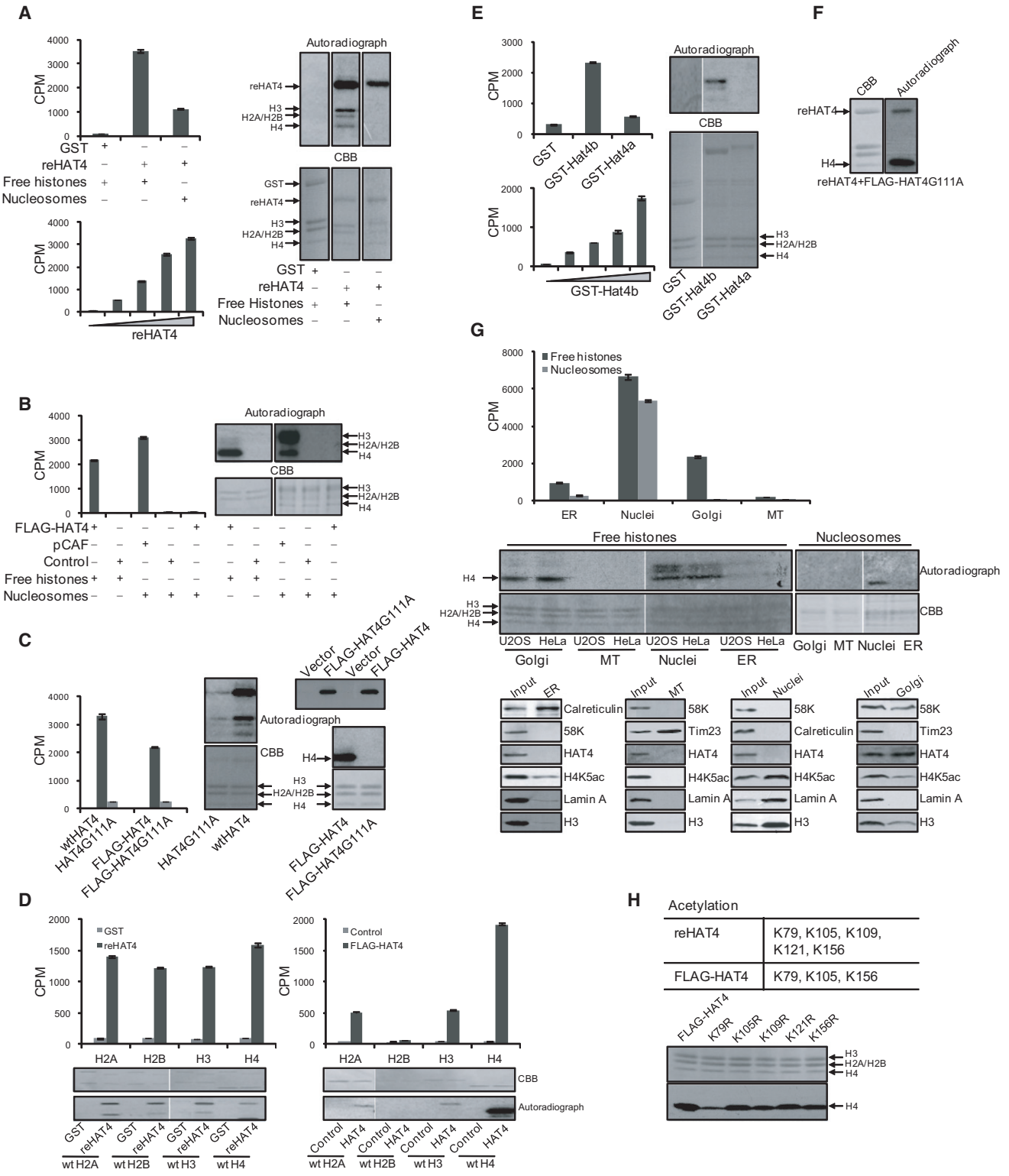

Figure 2. HAT4 Possesses HAT Activity toward Free, but Not Nucleosomal, Histones

(A and B) Bacterially expressed recombinant HAT4 (reHAT4) (A) or mammalian cell-purified HAT4 (B) was incubated with calf thymus histones or nucleosomes in the presence of [^{3}H]acetyl-CoA. The incorporation of [^{3}H]acetate was detected by liquid scintillation counting (left). The reactions were also resolved on SDS-PAGE followed by Coomassie Brilliant Blue (CBB) staining to detect total proteins and by autoradiography to detect [^{3}H]acetate-labeled proteins (right). Each bar represents the mean ± SD for three independent experiments. 0, 100 ng, 200 ng, 500 ng, or 1 μg reHAT4 were used.

Hat4a and Hat4b proteins, and tested their enzymatic activity. We found that Hat4b exhibited a HAT activity comparable to HAT4. However, Hat4a, which contains a 21-amino acid insertion in the N-acetyltransferase motif of Hat4b, appeared to harbor no HAT activity (Figure 2E).

It is interesting that reHAT4 acetylated all free histones while FLAG-HAT4 from mammalian cells had a clear preference for K20, K79, and K91 of histone H4. One possibility is that HAT4 requires one or more cofactors, which are missing from reHAT4, for its substrate specification. In order to test this hypothesis, we added FLAG-HAT4G111A immunoprecipitates from HeLa cells to reHAT4 and performed HAT activity assays in vitro. The results clearly indicated that reHAT4 in this condition selectively acetylated histone H4 (Figure 2F), supporting the argument that one or more cofactors exist in mammalian cells to assist the substrate specification of HAT4.

To support our proposition that HAT4 is anchored on the Golgi apparatus, we next fractionated the subcellular organelles/membrane vesicles of HeLa cells using the OptiPrep protocol (Sigma). The fractionated Golgi, mitochondria, endoplasmic reticulum, or nuclei were then incubated with calf thymus histones or nucleosomal histones in the presence of [^{3}H]acetyl-CoA. Liquid scintillation indicated that the endoplasmic reticulum and nuclei contained HAT activity and that the mitochondria had no HAT activity (Figure 2G), which were expected results. However, analysis of the Golgi fraction detected the presence of HAT activity (Figure 2G), supporting our argument that HAT4 exists on the Golgi apparatus.

Many HATs, incuding Rtt109 and CBP/p300 (Black et al., 2006; Karanam et al., 2006; Stavropoulos et al., 2008), are known to require autoacetylation for HAT activity. Indeed, bacterially purified HAT4 could acetylate itself in our experiments. We did not observe autoacetylation of FLAG-HAT4 in our system, possibly due to the small amount of mammalian cell-purified FLAG-HAT4. Analysis by mass spectrometry of the acetylation of reHAT4 and mammalian HAT4 indicated that mammalian HAT4 had K79, K105, and K156 acetylation, whereas reHAT4 contained K79, K105, K156, K109, and K121 acetylation (Figure 2H). Because of the presence of the overlapped acetylations between reHAT4 and mammalian HAT4 (K79, K105, and K156), we reasoned that mammalian HAT4 could also be autoacetylated. We then tested the HAT activity of FLAG-HAT4 mutants K79R, K105R, K109R, K121R, and K156R and found that HAT4K79R mutant exhibited a much weaker HAT activity (Figure 2H). We conclude that autoacetylation of HAT4 might be required for optimal HAT activity of HAT4.

HAT4 Mainly Targets H4K20, H4K79, and H4K91 for Acetylation

In order to determine if HAT4 exerts its enzymatic activity in a site-specific manner, recombinant full-length *Xenopus* histones were incubated with bacterially recombinant or mammalian cell-purified HAT4. The materials in the reactions were then analyzed by mass spectrometry. These experiments revealed that recombinant HAT4 targeted a variety of histone species and a broad spectrum of amino acid residues in vitro, including H4K5, H4K12, H4K20, H4K31, H4K77, H4K79, H4K91, H3K56, H3K122, H2BK34, H2BK46, and H2AK5, whereas HAT4 purified from mammalian cells mainly acetylated the lysine residues of histone H4, including H4K12, H4K20, H4K79, and H4K91 (Figure 3A).

To analyze the targeting sites of histones for HAT4 in vivo, the expression of HAT1 was knocked down in U2OS cells. The HAT1-depleted cells were then transfected with HAT4 siRNA, synchronized in S phase by double thymidine blocking. U2OS cells were also transfected with FLAG-HAT4 vectors, synchronized, and treated with trichostatin A (TSA), a histone deacetylase inhibitor. Histone modifications were analyzed by western blotting with specific antibodies. Due to the lack of appropriate antibodies against acetylated H4K20, H4K79, and H4K91, the soluble histones extracted from HAT4-depleted cells were also analyzed by mass spectrometry after being resolved on and retrieved from SDS-PAGE gels. The results from western blotting analysis indicated that, except for H2AK5, whose acetylation level was elevated in U2OS cells with HAT4 overexpression, all other tested histone acetylations showed undetectable changes (Figure 3B). The data obtained from mass spectrometry revealed that the levels of acetylated H4K20, H4K79, and H4K91 were markedly decreased in cells with HAT4 knockdown (Figure 3C); no changes in the acetylation levels of other lysine sites of histones were detected. The efficiency of HAT4 RNAi in cells treated with HAT4 siRNA or shRNA were examined by real-time RT-PCR, western blotting, or immunofluorescent imaging (Figure 3D). Together with our observations that mammalian HAT4

(C) Mutation of the conserved amino acid (glycine) in acetyl-CoA binding site of HAT4 resulted in the loss of its HAT activity. Bacterially expressed or mammalian cell-purified wild-type HAT4 and HAT4G111A mutant were incubated with calf thymus histones in the presence of [^{3}H]acetyl-CoA. The incorporation of [^{3}H] acetate was detected by liquid scintillation counting (left). The reaction mixtures were also resolved on SDS-PAGE followed by CBB staining to detect total proteins and by autoradiography to detect ^{3}H-acetylated proteins (right). Each bar represents the mean ± SD for three independent experiments.

(D) Experiments were performed as described in (A) and (B), except that recombinant wild-type *Xenopus* H2A, H2B, H3, and H4 were used as substrates. Each bar represents the mean ± SD for three independent experiments.

(E) *Drosophila* Hat4b but not Hat4a possess HAT activity. Experiments were performed as described in (C), except that bacterially expressed recombinant Hat4a and Hat4b was used. Each bar represents the mean ± SD for three independent experiments. 0, 100 ng, 200 ng, 500 ng, or 1 μg of GST-Hat4b were used.

(F) reHAT4 was incubated with calf thymus histones and [^{3}H]acetyl-CoA in the presence of FLAG-HAT4G111A-tranfected and anti-FLAG-purified cellular extracts. The reaction mixtures were resolved on SDS-PAGE followed by CBB staining and autoradiography.

(G) Golgi extracts display HAT activity. Subcellular organelles of HeLa cells–Golgi, mitochondria (MT), endoplasmic reticulum (ER), and nuclei–were extracted using the OptiPrep protocol. Calf thymus histones or nucleosomal histones were used as substrates for HAT assays. Each bar represents the mean ± SD for three independent experiments. Western blotting was performed using antibodies against the indicated proteins and the organelle-specific markers; 58K: Golgi; Calreticulin: ER; Tim23: MT; Lamin A: Nuclei.

(H) Acetylation of reHAT4 and FLAG-HAT4 identified by mass spectrometry. Different acetylation profiles were shown. In vitro HAT assays were performed as described in (A) and (B), except for using anti-FLAG-purified immunoprecipitates from FLAG-HAT4-, HAT4K79R-, HAT4K105R-, HAT4K109R-, HAT4K121R-, or HAT4K156R-transfected HeLa cells.

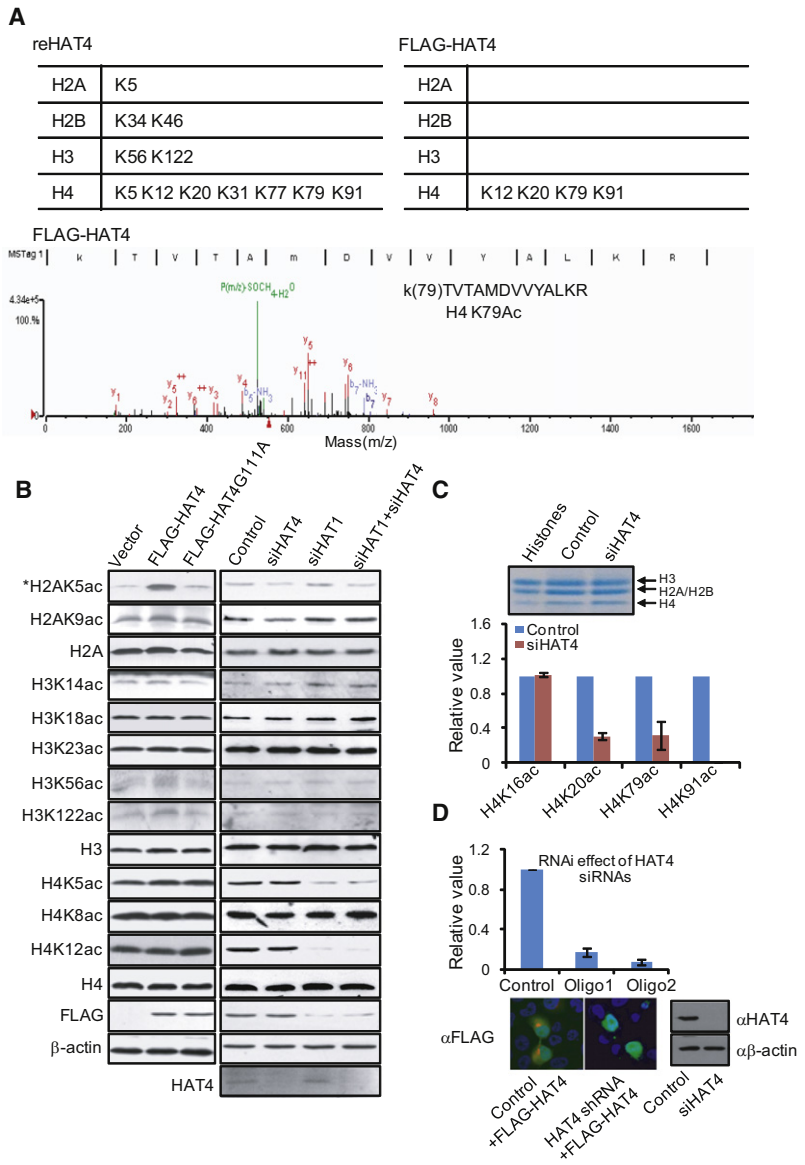

Figure 3. HAT4 Acetylates Free Histone H4 in a Site-Specific Manner

(A) Mass spectrometry analysis of lysine residues of histones acetylated by bacterially expressed HAT4 or mammalian cell-purified HAT4 with bacterially expressed *Xenopus* histones as substrates.

(B) The effect of overexpression or knockdown of HAT4 on histone acetylation in U2OS cells. U2OS cells were transfected with HAT4 or treated with HAT4 siRNA and/or HAT1 siRNA. The soluble histones were prepared and their acetylation levels were analyzed by western blotting.

(C) Mass spectrometry analysis of H4 acetylation by HAT4 in vivo. U2OS cells were treated with control or HAT4 siRNA. Cytoplasmic histones were extracted and resolved on SDS-PAGE followed by CBB staining. Histone bands were retrieved and analyzed by LC-MS-MS and MOLDI-MS-TOFF for acetylation modifications. Each bar represents the mean ± SD for three independent experiments.

(D) Verification of HAT4 knockdown in U2OS and MCF-7 cells by real-time RT PCR, western blotting, or immunofluorescent imaging. Each bar represents the mean ± SD for three independent experiments.

preferentially acetylated H4, we conclude that HAT4 mainly catalyzes the acetylation of free histone H4 at H4K20, H4K79, and H4K91 in vivo.

HAT4 Facilitates Nucleosome Assembly

The observation that HAT4 is able to acetylate H4K79 and H4K91 is intriguing. After all, the majority of histone acetylations, whether they are catalyzed by A-HAT or are deposited by B-HAT, are found in histone tails, whereas K79 and K91 reside in the globular domain of H4. Nevertheless, the globular domains of histones, due to their involvement in histone-histone interaction and octamer formation (Mersfelder and Parthun, 2006; Ye et al., 2005), are probably more pertinent than histone tails for nucleosome assembly. Therefore, in order to investigate if HAT4 facilitates replication-dependent chromatin assembly, we tested the supercoiling efficiency and micrococcal nuclease resistance of pSV011 plasmids in the presence of SV40 T antigen and radiolabeled nucleotide (α-^{32}P [dATP]) (Kamakaka et al., 1996; Kamakaka et al., 1994; Kaufman et al., 1995; Stillman and Gluzman, 1985) using human 293 S100 extracts under HAT4 and/or HAT1 knockdown. As shown in Figure 4A, in the presence of human chromatin assembly factor 1 (CAF-1), nucleosome assembly onto replicating DNA was more efficient with control cell extracts compared with extracts from cells with HAT1 or HAT4 knockdown. Densitometry analysis of autoradiogram lanes showed that supercoiling products decreased ~30% in siRNA-treated cells compared with control (Figure 4A, middle panel). Micrococcal nuclease resistance assays confirmed that the supercoiling was the result of nucleosome formation (Figure 4A, right panel), supporting the notion that HAT4 facilitates replication-coupled nucleosome assembly in vitro.

In order to further support this deduction, DNA micrococcal nuclease sensitivity assays (Lusser and Kadonaga, 2004) were performed to examine the formation of chromatin structure during replication in MCF-7 cells and U2OS cells in the absence of HAT4 in vivo. The results showed an increased sensitivity of DNAs to micrococcal nuclease digestion in HAT1-depleted cells and an even higher increase in HAT4-depleted cells compared with controls (Figure 4B). When nuclei from cells with coknockdown of HAT1 and HAT4 were digested, a much more dramatic increase in the sensitivity of DNAs to micrococcal nuclease was observed (Figure 4B). These results suggest that HAT4 impacts the global structure of chromatin, supporting a role for HAT4 in nucleosome formation and chromatin assembly. In addition, these results also suggest that HAT1 and HAT4 function cooperatively in the organization of the genome.

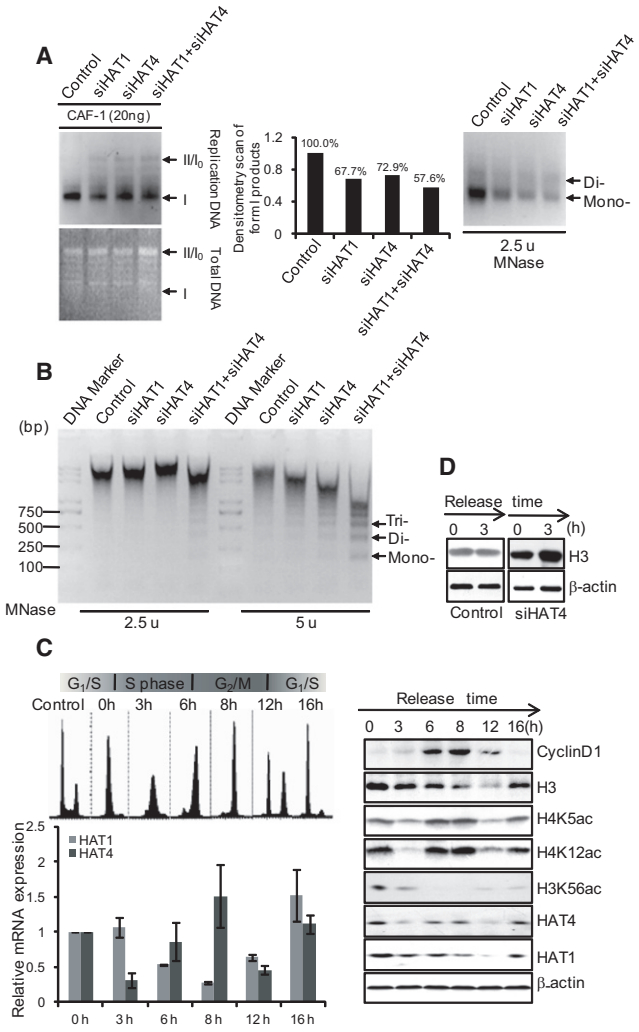

Figure 4. HAT4 Facilitates Proper Nucleosome Assembly

(A) HAT4 facilitates CAF-1-mediated nucleosome formation onto replicating DNA. Human 293 cells were treated with HAT1 and/or HAT4 siRNA. Plasmid pSV011 was replicated in siRNA-treated human 293 S100 extracts in the presence of T antigen, [α-^{32}P]-dATP, and CAF-1. Total DNA was visualized by ethidium bromide staining and by autoradiography. Migration of form I negatively supercoiled and form II/I_0 relaxed monomer circular DNA is indicated. Middle panel: Radioactively labeled supercoiled products were quantified by densitometry scan of the autoradiogram. Right panel: Micrococcal nuclease digestion analysis of chromatin assembled onto newly synthesized DNA. Mononucleosome (Mono-) and dinucleosome (Di-) are indicated.

(B) U2OS cells were treated with HAT1 siRNA and/or HAT4 siRNA, arrested by double thymidine block, and then released to S phase. Nuclei were then prepared and treated with 2.5 or 5 units/ml of MNase as indicated. Genomic DNA was purified and resolved by agarose gel electrophoresis. Mononucleosome (Mono-), dinucleosome (Di-), and trinucleosome (Tri-) are indicated.

(C) The expression profile of HAT4. HeLa cells were synchronized in S phase by double thymidine block, and the expression of HAT4 mRNA and protein were measured at the indicated times after release by real-time RT PCR and western blotting, respectively. Each bar represents the mean ± SD for three independent experiments.

(D) HAT4 knockdown led to the accumulation of soluble histones in cells. HeLa cells were synchronized in S phase by double thymidine block and released. Histone H3 expression levels were analyzed by western blotting with β-actin as internal control.

To further support the importance of HAT4 in chromatin assembly, the expressions of mRNA and protein of HAT4 and HAT1 were examined in HeLa cells that were synchronized with a double thymidine block before being released for cell cycling for different periods of time, representing different stages of the cell cycle. Notably, the expression patterns of HAT1 and HAT4 differed in the cell cycle, with the expression of HAT1 decreased and that of HAT4 increased during cell-cycle progression (Figure 4C). Also the expression of HAT1 peaked at the G_1/S boundary and that of HAT4 maximized at the S/G_2/M boundary (Figure 4C). In addition, knockdown of the expression of HAT4 resulted in an accumulation of soluble histones in the S phase in MCF-7 cells, probably reflecting impaired chromatin assembly (Figure 4D). Together with the substrate/site specificity of HAT1 and HAT4, the above experiments suggest that the two enzymes may have overlapping yet nonredundant activities.

Depletion of HAT4 Inhibits Cell Proliferation, Sensitizes Cells to DNA Damage, and Induces Cell Apoptosis

Defects in chromatin assembly, and thus in genome organization, would inevitably affect the growth and homeostasis of cells (Li et al., 2008). In order to investigate whether the involvement of HAT4 in nucleosome assembly could extend to a physiologically relevant cellular response, we determined the effect of loss-of-function of HAT4 on the growth and proliferation of MCF-7 cells. MCF-7 cells were treated with HAT1 siRNA and/or HAT4 siRNA. Twenty-four hours after the treatment, cells were split into 96-well plates and then harvested each day for 5 days for cell viability assays by Alamar blue staining (Nociari et al., 1998). Notably, knockdown of either HAT4 or HAT1 resulted in a significant decrease in cell number, and coknockdown of HAT1 and HAT4 had a more pronounced negative effect on cell proliferation (Figure 5A). In addition, HAT4-depleted MCF-7 cells were maintained in culture medium supplemented with 1 mg/ml G418 for 14 days and stained with crystal violet for colony counting (Shi et al., 2011; Sun et al., 2009). Colony numbers of HAT4-depleted cells decreased dramatically compared to control cells (Figure 5B). Further, the negative effect of HAT4 depletion on colony formation of MCF-7 cells could be partially rescued by overexpression of *Drosophila* Hat4b but not Hat4a (Figure 5B), which is consistent with our observation that *Drosophila* Hat4b, but not Hat4a, exhibited HAT activity.

Next, MCF-7 cells were synchronized in the G_0/G_1 phase by serum starvation, at the G_1/S boundary by double thymidine blocking, and at the M phase with nocodazole blocking. Cell-cycle profiling by flow cytometry indicated that, after release from serum starvation or from thymidine or nocodazole blocking, HAT4-depleted cells proceeded to cell cycle with a much lower efficiency and significantly slower kinetics compared to control cells (Figure 5C). Analogously, the effect of HAT4 depletion on MCF-7 cell cycling could be partially rescued by overexpression of *Drosophila* Hat4b but not Hat4a (Figure 5D). Collectively, these experiments suggest that HAT4 is required for normal cell proliferation and for proper cell-cycle progression and that its function depends on its HAT activity.

It is believed that defects in DNA replication-coupled nucleosome assembly are, at least in part, associated with an elevated sensitivity of cells to acute DNA damage (Li et al., 2008;

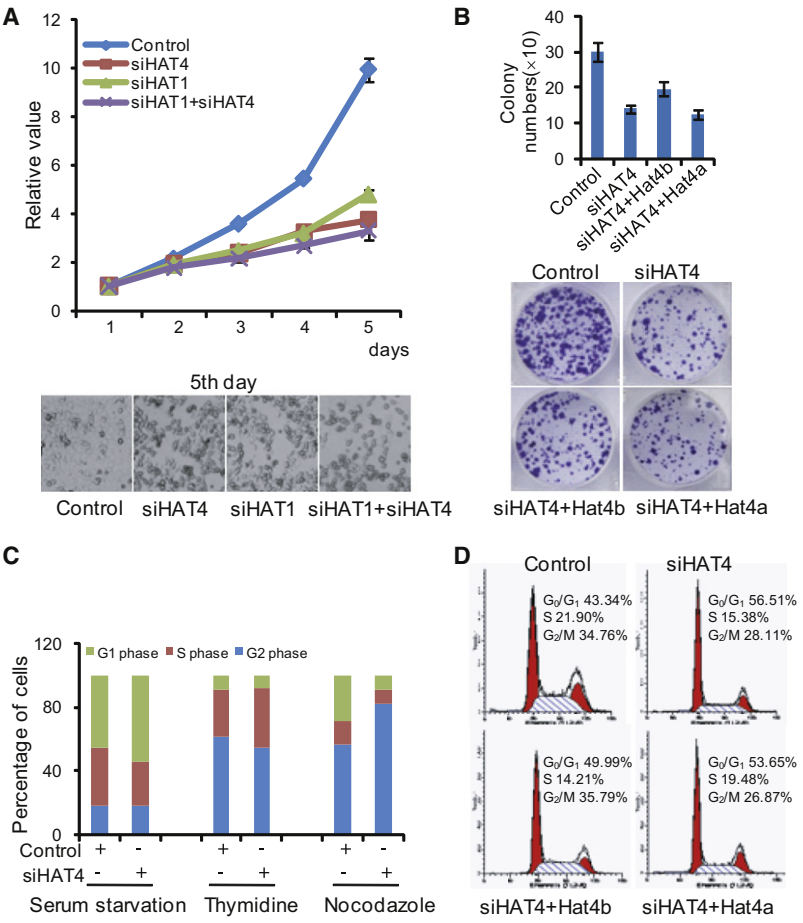

Figure 5. Depletion of HAT4 Inhibits Cell Growth

(A) Depletion of HAT4 is associated with inhibition of cell proliferation. Control or HAT1 and/or HAT4 siRNA-treated MCF-7 cells were split into 96-well plates and then harvested at day 1, 2, 3, 4, or 5. The growth curves of the cells were measured by Alamar blue cell viability assays. Each point represents the mean ± SD for three independent experiments.

(B) Hat4b but not Hat4a partially rescued the effect of HAT4 knockdown. MCF-7 cells were transfected with pGCsi-Nonsilencer, pGCsi-HAT4 shRNA, pGCSi-HAT4 shRNA plus pcDNA3.1-FLAG-Hat4a, or pGCSi-HAT4 shRNA plus pcDNA3.1-FLAG-Hat4b. Cells were maintained in G418-containing medium for 14 days before staining with crystal violet and counting for colony numbers. Each bar represents the mean ± SD for three independent experiments.

(C) MCF-7 cells treated with control siRNA or HAT4 siRNA were synchronized by serum starvation, double thymidine block, or thymidine nocodazole block at G_0/G_1, G_1/S, or the G_2/M boundary, respectively. Cell-cycle progression after releasing was analyzed by flow cytometry.

(D) Hat4b but not Hat4a could partially rescue the delay of the cell cycle associated with HAT4 knockdown. MCF-7 cells were transfected with control, HAT4 shRNA, HAT4 shRNA plus Hat4a, or HAT4 shRNA plus Hat4b. Transfected cells were subjected to cell-cycle analysis by flow cytometry.

Masumoto et al., 2005). In order to further support the role of HAT4 in nucleosome assembly, HAT4-depleted U2OS cells were subjected to DNA-damaging sensitivity assays. In these experiments, U2OS cells were treated with HAT1 siRNA and/or HAT4 siRNA, challenged with various DNA-damaging agents including UV irradiation, hydroxyurea, and camptothecin (CPT), and examined for viability by Alamar blue staining. The results showed that, after insults by either the double-stranded (camptothecin and hydroxyurea) or single-stranded DNA-damaging agents (UV radiation) (Kleiman et al., 1990), loss-of-function of HAT4 was associated with a significant decrease in the number of viable U2OS cells, and coknockdown of HAT1 and HAT4 resulted in a more marked reduction in the cell number (Figure 6A). These results suggest that HAT4 depletion is associated with an increased sensitivity of cellular DNA to DNA damage.

The decreased cell numbers and increased sensitivity to DNA damage of the HAT4-deficient cells described above could be the result of cell death due to the inability of the cells to properly organize their genome or a reflection of cell apoptosis due to HAT4 deficiency-induced stress. In order to further explore the cellular function of HAT4, we examined the effect of HAT4 knockdown on cell apoptosis. For this purpose, U2OS cells were treated with HAT1 siRNA and/or HAT4 siRNA, synchronized to the S phase by a double thymidine block, and then double stained with annexin V and propidium iodide. Flow cytometry analysis revealed that knockdown of HAT1 or HAT4 resulted in a ~25% or ~30% increase in the number of U2OS cells that underwent apoptosis, respectively; coknockdown of HAT1 and HAT4 led to a even higher percentage of U2OS cells undergoing apoptosis (Figure 6B). In support of these observations, western blotting analysis indicated that HAT4-deficient cells exhibited an increased level of p53 protein and an elevated level of H2AX phosphorylation (Figure 6B, lower panel), indicative of the activation of the apoptotic response in these cells. Collectively, all of these experiments support the notion that HAT4 is critically involved in proper chromatin assembly and normal cell functioning.

DISCUSSION

Posttranslational modifications of histones are important for histone import, nucleosome formation/chromatin assembly, and chromatin functions (Strahl and Allis, 2000). The identification of enzymes that catalyze these modifications will thus be essential for understanding the organization and functions of the chromatin fiber. In past decades, numerous proteins have been shown to catalyze the modification of histones through various enzymatic reactions including phosphorylation, acetylation, methylation, glycosylation, ubiquitylation, sumoylation, and polyribosylation (Kouzarides, 2007). Among these proteins, HATs, which are responsible for the addition of the acetyl moieties to histones, represent one of the most extensively studied groups of histone modifiers (Lahn et al., 2002). However, a vast

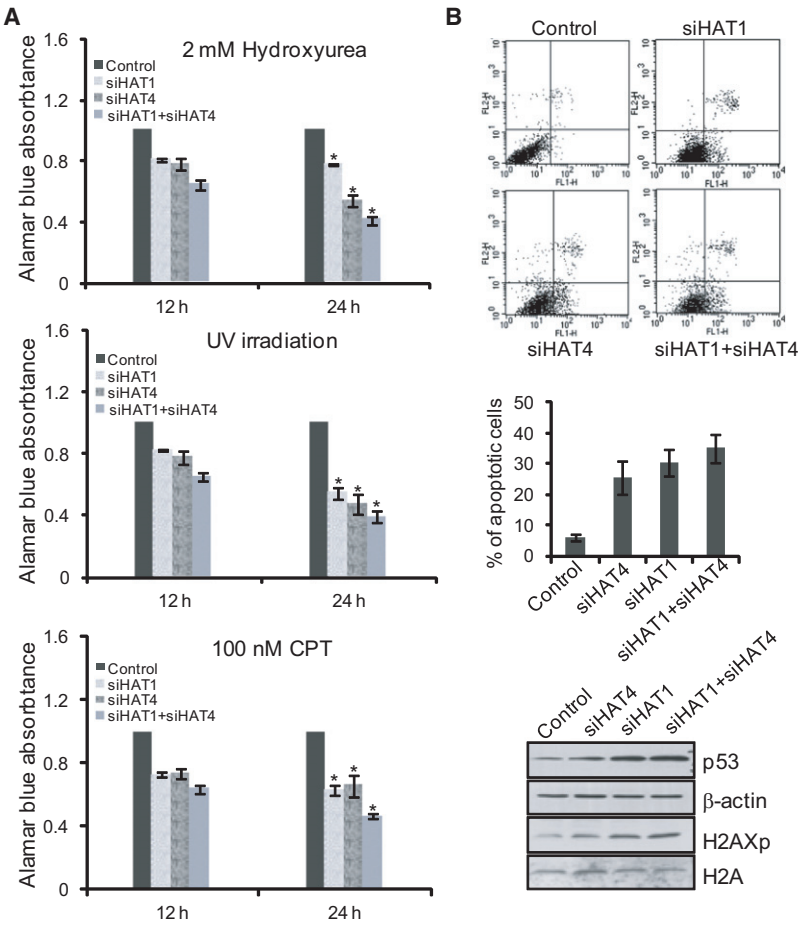

Figure 6. Depletion of HAT4 Sensitizes Cells to DNA Damage and Induces Apoptosis

(A) U2OS cells were treated with control siRNA or HAT1 siRNA and/or HAT4 siRNA. Thirty-two hours later, cells were treated with UV irradiation, 2 mM hydroxyurea, or 100 nM CPT for 12 or 24 hr followed by Alamar blue staining to detect their viability. Each bar represents the mean ± SD for three independent experiments. Post hoc tests were performed in conjunction with one-way ANOVA using SPSS 17.0 software for statistical analysis. Stars indicate that the differences of those groups are significant compared with the control ($p < 0.01$).

(B) HAT4 knockdown promotes cell apoptosis. siRNA-treated U2OS cells were double stained with annexin V and propidium iodide. Cell apoptosis was determined by flow cytometry. Each bar represents the mean ± SD for three independent experiments. The protein levels of p53 and H2AXP-S139 in siRNA-treated and double thymidine-synchronized U2OS cells were measured by western blotting.

majority of these HATs are so-called A-HATs, which target the nucleosomal histones and function in the regulation of gene transcription. In contrast, histone acetyltransferases, which are responsible for modifying newly synthesized histones that are yet to be incorporated into chromatin (B-HATs) have received less attention. It is reported that HAT1, a B-HAT, is responsible for the acetylation of newly synthesized histone H4 at K5 and K12 and is involved in de novo chromatin assembly (Parthun et al., 1996). However, yeast with *HAT1* ablation exhibited no apparent defects in cell growth (Ruiz-García et al., 1998), and chicken DT40 cells with homozygous *HAT1* deletion retained high levels of H4K5 and H4K12 acetylation in the soluble histone fraction (Barman et al., 2006). These genetic studies strongly suggest that HAT1 may not be the only enzyme involved in the acetylation of newly synthesized histone H4. Considering the emerging evidence that acetylation also occurs on other lysine residues of H4, such as H4K8 and H4K91 (Verreault et al., 1996; Ye et al., 2005), it is becoming clear that additional B-HATs that act on newly synthesized histones do indeed exist.

In the current report, we describe a member of the human GCN5-related N-acetyltransferases and another B-HAT, HAT4. We showed that HAT4 catalyzes the acetylation of free but not nucleosomal histones in vitro and in vivo. Interestingly, we found that reHAT4 acetylated all free histones while FLAG-HAT4 from mammalian cells had a substrate preference for K20, K79, and K91 of histone H4. One reason for this discrepancy might be that HAT4 requires one or more cofactors, which are present in mammalian cells but missing in bacteria, for its substrate specification. Although affinity purification with GST-HAT4 and immunopurification with FLAG-HAT4 coupled with mass spectrometry identified no potential candidates as HAT4's cofactor(s), due to the resolution limitation of these experiments, the existence of such cofactor(s) is still likely. Indeed, addition of FLAG-HAT4G111A immunoprecipitates from HeLa cells to reHAT4 conferred on reHAT the substrate selectivity, supporting the existence of HAT4 cofactor(s) in mammalian cells.

For nearly four decades, the study of histone modifications has largely focused on those that occur on the tails of the core histones. However, recent studies by mass spectrometry have identified over 30 sites of histone methylation and acetylation, with a majority of these localized in the core globular histone domains (Mersfelder and Parthun, 2006; Zhang et al., 2002; Zhang et al., 2003). While the data concerning these modifications are still limited, current evidence indicates that they may be of great physiological relevance and suggest that histone core domain modifications may turn out to be as important as modifications within histone tails (Zhang et al., 2002; Zhang et al., 2003). In addition, crystal structure studies of nucleosomes have revealed that histone modifications in the globular domains occupy the soluble and accessible faces, the histone lateral surfaces, or the histone-histone interfaces of nucleosomes (Cosgrove et al., 2004; Freitas et al., 2004). Therefore, it is likely that the modifications deposited in the globular domains may be more important to the formation of the hierarchical architecture of the chromatin fiber.

Our experiments indicate that HAT4 acetylates H4K20, H4K79, and H4K91 in vivo. Considering the fact that the well-accepted substrates of H4K5 and H4K12 for HAT1 were located

within the region of the corresponding histone tail, while H4K20, H4K79, and H4K91 reside near or in the globular domain of H4, it appears that HAT1 is responsible for the acetylation of the H4 tail, whereas HAT4 is responsible for the acetylation of the H4 core. If this interpretation is correct, it means that HAT1 and HAT4 differ functionally, at least in substrate specifications. In support of this argument, we found that the expression patterns of HAT1 and HAT4 differed during the progression of the cell cycle, with HAT4, but not HAT1, accumulating at the $S/G_2/M$ phase when new histones are synthesized/modified and chromatin is assembled.

We showed that HAT4 is localized to the Golgi apparatus. This organelle is considered to be a distribution and shipment center because of its function of preparing proteins and lipids for export out of the cell or transport to other locations inside the cell (Andreeva et al., 1998; Wilson et al., 2011). This function of the Golgi apparatus has been associated with a variety of enzymatic activities including protease, glycosylase, acetyltransferase, phospholipase, and lipid phosphate phosphatase that have been identified in this organelle (Fernández-Hernando et al., 2006; Freyberg et al., 2003; Sciorra and Morris, 2002). However, to date, no HAT activity has been reported in the Golgi apparatus. Although modification of newly synthesized histones by acetylation in the Golgi apparatus is consistent with the general function of this organelle, the observation that HAT4 is localized on the Golgi apparatus is still intriguing, in that it links the function of the Golgi apparatus to chromatin biology.

De novo assembly of chromatin in mammalian cells is a complex, multistep process, and the overall pattern of free histone acetylation is markedly diverse. Obviously, there is much to be learned about the mechanisms employed by eukaryotic cells to control the modification status of the lateral surface of nucleosomes. Perhaps more relevant to our current report, despite characterization of the substrate specificity of HAT1 and HAT4, functional differentiation between these two B-HATs is still not clear. Nonetheless, our data indicate that HAT4 is a member of the GNAT superfamily of histone acetyltransferases and that it mainly catalyzes the acetylation of the core domain of newly synthesized histone H4 and is critically involved in nucleosome assembly and chromatin stability.

EXPERIMENTAL PROCEDURES

Histone Acetyltransferase Assay

The histone acetyltransferase activities of recombinant HAT4 or immunoprecipitated FLAG-HAT4 were determined as described elsewhere (Ait-Si-Ali et al., 1998; Han et al., 2007). Briefly, samples were incubated at 30°C for 30 min in 15 μl reaction mixtures that contained 50 mM Tris-HCl (pH 8.0), 5% (w/v) glycerol, 0.1 mM EDTA, 1 mM dithiothreitol, 5 mM PMSF, and 6 pmol of [^{3}H]acetyl-CoA (4.3 mCi/mmol; Amersham Biosciences). After incubation at 30°C for 30 min, one half of the products (7.5 μl) was measured by scintillation counting. Products left were first resolved using 15% SDS-PAGE, and then gels were dried and exposed to films to detect which protein was acetylated.

Soluble Histone Purification

Soluble histones were obtained as described (Schultz et al., 1997) with minor modification. Briefly, cytoplasmic extracts were prepared from mock or HAT4 siRNA-treated HeLa cells. Extracts were mixed on ice with 4 N HCl to a final concentration of 0.4 N and then spun for 10 min at 4200 × g. Perchloric acid (70%) was added to the supernatant, making a 1:10 dilution to precipitate soluble histones. Histones recovered from the extract (85%–95% pure) exist in multiple states of posttranslational modification (Schultz et al., 1997). Histone bands were cut, digested with trypsin (Sigma), and analyzed by LC-MS-MS or MOLDI-MS-TOFF for their modifications.

SV40 DNA Replication-Coupled Nucleosome Assembly Assay

Recombinant human CAF-1 and SV40 T antigen were produced in insect cells and purified as previously described (Kaufman et al., 1995; Lanford, 1988; Simanis and Lane, 1985; Verreault et al., 1996). The S100 extracts for SV40 DNA replication were prepared from control or HAT1 and/or HAT4 siRNA-treated human 293 cells and the assays were performed as previously described (Kamakaka et al., 1996; Kamakaka et al., 1994; Stillman and Gluzman, 1985). Reaction mixtures (50 μl) contained 40 mM HEPES-KOH (pH 7.5), 8 mM $MgCl_2$, 0.5 mM dithiothreitol, 100 μM each of dTTP, dGTP, and dCTP, 25 μM [α-^{32}P]dATP (1000 cpm/pmol), 3 mM ATP, 200 μM each of CTP, UTP, and GTP, 40 mM creatine phosphate, 1 μg creatine phosphokinase, 0.3 μg pSV40 DNA, 0.5 μg T antigen, and 175 to 200 μg of equal amount S100 extracts of siRNA treated cells. DNA replication reactions were carried out at 37°C for 120 min in the presence of CAF-1. The supercoiled products were either treated with micrococcal nuclease or terminated by 10 mM EDTA. DNA products were purified, resolved on 1.25% or 2% native agarose gels, stained with EB, and dried for autoradiograph.

MNase Sensitivity Assay

Cells were treated with control siRNA or with HAT1 siRNA and/or HAT4 siRNA. Cells were then synchronized in S phase by double thymidine blocking and collected. Permeabilized nuclei were prepared and digested with MNase. Genomic DNA was purified and electrophoresed on 2% agarose gels.

SUPPLEMENTAL INFORMATION

Supplemental Information includes Supplemental Experimental Procedures and Supplemental References and can be found with this article online at doi:10.1016/j.molcel.2011.07.032.

ACKNOWLEDGMENTS

We thank Di Miao (Tsinghua University, China) for assisting in mass spectrometry analysis. This work was supported by grants (30830032 and 30921062 to Y.S.; 30800560 to X.Y.) from the National Natural Science Foundation of China and grants (973 Program: 2011CB504204 and 2007CB914503 to Y.S.) from the Ministry of Science and Technology of China.

Received: March 15, 2011
Revised: May 23, 2011
Accepted: July 6, 2011
Published: October 6, 2011

REFERENCES

Ait-Si-Ali, S., Ramirez, S., Robin, P., Trouche, D., and Harel-Bellan, A. (1998). A rapid and sensitive assay for histone acetyl-transferase activity. Nucleic Acids Res. *26*, 3869–3870.

Andreeva, A.V., Kutuzov, M.A., Evans, D.E., and Hawes, C.R. (1998). The structure and function of the Golgi apparatus: a hundred years of questions. J. Exp. Bot. *49*, 1281–1291.

Barman, H.K., Takami, Y., Ono, T., Nishijima, H., Sanematsu, F., Shibahara, K., and Nakayama, T. (2006). Histone acetyltransferase 1 is dispensable for replication-coupled chromatin assembly but contributes to recover DNA damages created following replication blockage in vertebrate cells. Biochem. Biophys. Res. Commun. *345*, 1547–1557.

Black, J.C., Choi, J.E., Lombardo, S.R., and Carey, M. (2006). A mechanism for coordinating chromatin modification and preinitiation complex assembly. Mol. Cell *23*, 809–818.

Burgess, R.J., Zhou, H., Han, J., and Zhang, Z. (2010). A role for Gcn5 in replication-coupled nucleosome assembly. Mol. Cell *37*, 469–480.

Cosgrove, M.S., Boeke, J.D., and Wolberger, C. (2004). Regulated nucleosome mobility and the histone code. Nat. Struct. Mol. Biol. *11*, 1037–1043.

Dutnall, R.N., Tafrov, S.T., Sternglanz, R., and Ramakrishnan, V. (1998). Structure of the histone acetyltransferase Hat1: a paradigm for the GCN5-related N-acetyltransferase superfamily. Cell *94*, 427–438.

Fernández-Hernando, C., Fukata, M., Bernatchez, P.N., Fukata, Y., Lin, M.I., Bredt, D.S., and Sessa, W.C. (2006). Identification of Golgi-localized acyl transferases that palmitoylate and regulate endothelial nitric oxide synthase. J. Cell Biol. *174*, 369–377.

Fillingham, J., Recht, J., Silva, A.C., Suter, B., Emili, A., Stagljar, I., Krogan, N.J., Allis, C.D., Keogh, M.C., and Greenblatt, J.F. (2008). Chaperone control of the activity and specificity of the histone H3 acetyltransferase Rtt109. Mol. Cell. Biol. *28*, 4342–4353.

Freitas, M.A., Sklenar, A.R., and Parthun, M.R. (2004). Application of mass spectrometry to the identification and quantification of histone post-translational modifications. J. Cell. Biochem. *92*, 691–700.

Freyberg, Z., Siddhanta, A., and Shields, D. (2003). "Slip, sliding away": phospholipase D and the Golgi apparatus. Trends Cell Biol. *13*, 540–546.

Fujiwara, T., Oda, K., Yokota, S., Takatsuki, A., and Ikehara, Y. (1988). Brefeldin A causes disassembly of the Golgi complex and accumulation of secretory proteins in the endoplasmic reticulum. J. Biol. Chem. *263*, 18545–18552.

Ge, Z., Wang, H., and Parthun, M.R. (2011). Nuclear Hat1p complex (NuB4) components participate in DNA repair-linked chromatin reassembly. J. Biol. Chem. *286*, 16790–16799.

Han, J., Zhou, H., Horazdovsky, B., Zhang, K., Xu, R.M., and Zhang, Z. (2007). Rtt109 acetylates histone H3 lysine 56 and functions in DNA replication. Science *315*, 653–655.

Kamakaka, R.T., Kaufman, P.D., Stillman, B., Mitsis, P.G., and Kadonaga, J.T. (1994). Simian virus 40 origin- and T-antigen-dependent DNA replication with Drosophila factors in vitro. Mol. Cell. Biol. *14*, 5114–5122.

Kamakaka, R.T., Bulger, M., Kaufman, P.D., Stillman, B., and Kadonaga, J.T. (1996). Postreplicative chromatin assembly by Drosophila and human chromatin assembly factor 1. Mol. Cell. Biol. *16*, 810–817.

Karanam, B., Jiang, L., Wang, L., Kelleher, N.L., and Cole, P.A. (2006). Kinetic and mass spectrometric analysis of p300 histone acetyltransferase domain autoacetylation. J. Biol. Chem. *281*, 40292–40301.

Kaufman, P.D., Kobayashi, R., Kessler, N., and Stillman, B. (1995). The p150 and p60 subunits of chromatin assembly factor I: a molecular link between newly synthesized histones and DNA replication. Cell *81*, 1105–1114.

Kleiman, N.J., Wang, R.R., and Spector, A. (1990). Ultraviolet light induced DNA damage and repair in bovine lens epithelial cells. Curr. Eye Res. *9*, 1185–1193.

Kouzarides, T. (2007). SnapShot: Histone-modifying enzymes. Cell *128*, 802.

Lahn, B.T., Tang, Z.L., Zhou, J., Barndt, R.J., Parvinen, M., Allis, C.D., and Page, D.C. (2002). Previously uncharacterized histone acetyltransferases implicated in mammalian spermatogenesis. Proc. Natl. Acad. Sci. USA *99*, 8707–8712.

Lanford, R.E. (1988). Expression of simian virus 40 T antigen in insect cells using a baculovirus expression vector. Virology *167*, 72–81.

Li, Q., Zhou, H., Wurtele, H., Davies, B., Horazdovsky, B., Verreault, A., and Zhang, Z. (2008). Acetylation of histone H3 lysine 56 regulates replication-coupled nucleosome assembly. Cell *134*, 244–255.

Lu, L., Berkey, K.A., and Casero, R.A., Jr. (1996). RGFGIGS is an amino acid sequence required for acetyl coenzyme A binding and activity of human spermidine/spermine N1acetyltransferase. J. Biol. Chem. *271*, 18920–18924.

Luger, K., Rechsteiner, T.J., Flaus, A.J., Waye, M.M., and Richmond, T.J. (1997). Characterization of nucleosome core particles containing histone proteins made in bacteria. J. Mol. Biol. *272*, 301–311.

Lusser, A., and Kadonaga, J.T. (2004). Strategies for the reconstitution of chromatin. Nat. Methods *1*, 19–26.

Masumoto, H., Hawke, D., Kobayashi, R., and Verreault, A. (2005). A role for cell-cycle-regulated histone H3 lysine 56 acetylation in the DNA damage response. Nature *436*, 294–298.

Mersfelder, E.L., and Parthun, M.R. (2006). The tale beyond the tail: histone core domain modifications and the regulation of chromatin structure. Nucleic Acids Res. *34*, 2653–2662.

Nociari, M.M., Shalev, A., Benias, P., and Russo, C. (1998). A novel one-step, highly sensitive fluorometric assay to evaluate cell-mediated cytotoxicity. J. Immunol. Methods *213*, 157–167.

Parthun, M.R. (2007). Hat1: the emerging cellular roles of a type B histone acetyltransferase. Oncogene *26*, 5319–5328.

Parthun, M.R., Widom, J., and Gottschling, D.E. (1996). The major cytoplasmic histone acetyltransferase in yeast: links to chromatin replication and histone metabolism. Cell *87*, 85–94.

Richman, R., Chicoine, L.G., Collini, M.P., Cook, R.G., and Allis, C.D. (1988). Micronuclei and the cytoplasm of growing Tetrahymena contain a histone acetylase activity which is highly specific for free histone H4. J. Cell Biol. *106*, 1017–1026.

Ruiz-García, A.B., Sendra, R., Galiana, M., Pamblanco, M., Pérez-Ortín, J.E., and Tordera, V. (1998). HAT1 and HAT2 proteins are components of a yeast nuclear histone acetyltransferase enzyme specific for free histone H4. J. Biol. Chem. *273*, 12599–12605.

Saraste, J., Palade, G.E., and Farquhar, M.G. (1987). Antibodies to rat pancreas Golgi subfractions: identification of a 58-kD cis-Golgi protein. J. Cell Biol. *105*, 2021–2029.

Schultz, M.C., Hockman, D.J., Harkness, T.A., Garinther, W.I., and Altheim, B.A. (1997). Chromatin assembly in a yeast whole-cell extract. Proc. Natl. Acad. Sci. USA *94*, 9034–9039.

Sciorra, V.A., and Morris, A.J. (2002). Roles for lipid phosphate phosphatases in regulation of cellular signaling. Biochim. Biophys. Acta *1582*, 45–51.

Shi, L., Sun, L., Li, Q., Liang, J., Yu, W., Yi, X., Yang, X., Li, Y., Han, X., Zhang, Y., et al. (2011). Histone demethylase JMJD2B coordinates H3K4/H3K9 methylation and promotes hormonally responsive breast carcinogenesis. Proc. Natl. Acad. Sci. USA *108*, 7541–7546.

Simanis, V., and Lane, D.P. (1985). An immunoaffinity purification procedure for SV40 large T antigen. Virology *144*, 88–100.

Sklenar, A.R., and Parthun, M.R. (2004). Characterization of yeast histone H3-specific type B histone acetyltransferases identifies an ADA2-independent Gcn5p activity. BMC Biochem. *5*, 11.

Stavropoulos, P., Nagy, V., Blobel, G., and Hoelz, A. (2008). Molecular basis for the autoregulation of the protein acetyl transferase Rtt109. Proc. Natl. Acad. Sci. USA *105*, 12236–12241.

Stillman, B.W., and Gluzman, Y. (1985). Replication and supercoiling of simian virus 40 DNA in cell extracts from human cells. Mol. Cell. Biol. *5*, 2051–2060.

Strahl, B.D., and Allis, C.D. (2000). The language of covalent histone modifications. Nature *403*, 41–45.

Sun, L., Shi, L., Li, W., Yu, W., Liang, J., Zhang, H., Yang, X., Wang, Y., Li, R., Yao, X., et al. (2009). JFK, a Kelch domain-containing F-box protein, links the SCF complex to p53 regulation. Proc. Natl. Acad. Sci. USA *106*, 10195–10200.

Verreault, A., Kaufman, P.D., Kobayashi, R., and Stillman, B. (1996). Nucleosome assembly by a complex of CAF-1 and acetylated histones H3/H4. Cell *87*, 95–104.

Wang, Y., Zhang, H., Chen, Y., Sun, Y., Yang, F., Yu, W., Liang, J., Sun, L., Yang, X., Shi, L., et al. (2009). LSD1 is a subunit of the NuRD complex and targets the metastasis programs in breast cancer. Cell *138*, 660–672.

Wilson, C., Venditti, R., Rega, L.R., Colanzi, A., D'Angelo, G., and De Matteis, M.A. (2011). The Golgi apparatus: an organelle with multiple complex functions. Biochem. J. *433*, 1–9.

Wolf, E., Vassilev, A., Makino, Y., Sali, A., Nakatani, Y., and Burley, S.K. (1998). Crystal structure of a GCN5-related N-acetyltransferase: Serratia marcescens aminoglycoside 3-N-acetyltransferase. Cell *94*, 439–449.

Wu, H., Chen, Y., Liang, J., Shi, B., Wu, G., Zhang, Y., Wang, D., Li, R., Yi, X., Zhang, H., et al. (2005). Hypomethylation-linked activation of PAX2 mediates tamoxifen-stimulated endometrial carcinogenesis. Nature *438*, 981–987.

Ye, J., Ai, X., Eugeni, E.E., Zhang, L., Carpenter, L.R., Jelinek, M.A., Freitas, M.A., and Parthun, M.R. (2005). Histone H4 lysine 91 acetylation a core domain modification associated with chromatin assembly. Mol. Cell *18*, 123–130.

Zhang, K., Tang, H., Huang, L., Blankenship, J.W., Jones, P.R., Xiang, F., Yau, P.M., and Burlingame, A.L. (2002). Identification of acetylation and methylation sites of histone H3 from chicken erythrocytes by high-accuracy matrix-assisted laser desorption ionization-time-of-flight, matrix-assisted laser desorption ionization-postsource decay, and nanoelectrospray ionization tandem mass spectrometry. Anal. Biochem. *306*, 259–269.

Zhang, L., Eugeni, E.E., Parthun, M.R., and Freitas, M.A. (2003). Identification of novel histone post-translational modifications by peptide mass fingerprinting. Chromosoma *112*, 77–86.